Applied Catalysis A: General 489 (2015) 203–208

Contents lists available at ScienceDirect

Applied Catalysis A: General

journal homepage: www.elsevier.com/locate/apcata

Highly effective continuous-flow monolithic silica microreactors for acid catalyzed processes

A. Koreniuk[a], K. Maresz[a], K. Odrozek[b], A.B. Jarzębski[a,b], J. Mrowiec-Białoń[a,b,*]

[a] Institute of Chemical Engineering, Polish Academy of Sciences, Bałtycka 5, 44-100 Gliwice, Poland
[b] Department of Chemical Engineering and Process Design, Silesian University of Technology, Ks. M. Strzody 7, 44-100 Gliwice, Poland

ARTICLE INFO

Article history:
Received 28 August 2014
Received in revised form 21 October 2014
Accepted 23 October 2014
Available online 1 November 2014

Keywords:
Microreactors
Silica monoliths
Acid catalysis
Esterification
Hierarchical materials

ABSTRACT

This work reports the performance of a new monolithic silica microreactor, activated with sulphonic acid groups in the continuous-flow synthesis of *n*-butyl acetate and *n*-butyl lactate. A reactive core of the reactor was made of a single silica rod with bi-continuous structure, containing flow-through pores with diameter in the range of 20–50 μm and mesopores of ca. 20 nm localized in silica struts. This structure resulted in low pressure drop, even at flow rates large enough to eliminate external mass transfer effect on the reaction kinetics. The microreactor functionalized with 0.65 mmol/g of $-SO_3H$ groups showed high activity and productivity in both esterification reactions carried out in temperatures up to 140 °C. Structural and catalytic stability of the microreactor was confirmed to demonstrate its process viability.

1. Introduction

Synthesis of most fine chemicals is typically carried out in a liquid phase and batch operation. Their replacement by continuous processes using microreactor-based technologies can make them more effective, safer and to give products with stable properties. Catalysts beads, currently applied as column reactor packings in fine chemicals' synthesis, are usually of 50–100 μm diameter. Therefore, their application often leads to serious operational problems; excessive backpressure results in a maldistribution of fluids, and thus formation of stagnant zones and hot spots, which in addition to a fairly long diffusion path, leads to lower yields, poorer selectivity and reduced catalyst life [1]. Continuous-flow monolithic polymeric microreactors show important advantages: defined system of flow-through pores and facile modification of the surface using ample arsenals of chemical tools [2,3]. But their thermal sensitivity and propensity to swell are serious drawbacks [4]. Typical ceramic (e.g. cordierite) monoliths, which feature bunch of channels of 1–5 mm sizes, connected with smaller ones of ca. 0.1–1.0 mm, are aimed at gas-phase reactions [5].

Silica-based continuous-flow monolithic microreactors, first proposed by the Montpellier group, appeared to be extremely promising for the cost-effective production of fine chemicals [6]. This stems from a unique, bi-continuous structure of the monoliths in which flow-through macropores are connected to an extensive network of meso- and micro-pores present in the silica skeleton [6–8]. In effect, pressure drops are fairly small, even at considerable throughputs, whereas easily accessible large surface area offers very large concentration of active sites per unit volume. Initially, such microreactor was made of a single monolith–MonoSil, the surface of which was functionalized with $-NH_2$ or $-HSO_3$ groups [6]. Control of its meso- and macro-porosity was obtained by combining phase separation method, elaborated by Nakanishi [9–11], with pseudomorphic synthesis [12,13], to obtain an ordered mesoporosity of the silica skeleton. But more importantly perhaps, the productivity of MonoSil microreactors in Knovenagel reaction and acid transesterification was shown to be 13 and 18 times larger than in the corresponding batch processes.

The original Nakanishi method was later modified [14,15] to give silica monoliths with notably larger macropores (30–50 μm) and more isotropic structure. Their pore structure was not destroyed after immobilization of ionic liquids and the catalysts obtained from the crushed monoliths were very active, selective and stable in the Baeyer–Villiger reaction and also in aerobic oxidation of primary alcohols [16–18].

The up to date methods of silica modification [19] offer huge potentials to develop microreactors with the structure

---

[*] Corresponding author at: Polish Academy of Sciences, Institute of Chemical Engineering, Bałtycka 5, 44-100 Gliwice, Poland. Tel.: +48 32 2310811; fax: +48 32 2310318.
E-mail address: jmrowiec@polsl.pl (J. Mrowiec-Białoń).

http://dx.doi.org/10.1016/j.apcata.2014.10.047
0926-860X/

purposely designed to meet specific catalytic and process engineering demands. Most recently these monoliths were successfully converted into a miniaturized multichannel enzymatic reactor [20] which could operate at flow rates up to about 20 cm^3/min at backpressure not exceeding 2.5 bar. Worth noting, the sucrose hydrolysis catalysed by invertase appeared to proceed in this microreactor with maximum rate over 1000 times faster than in the MCF-based slurry system, and the enzyme confined in mesopores showed notably larger affinity to substrate than the native one, a clear signature of hyperactivity effect.

For this reason we deemed it important to test the potentials of continuous-flow microreactors made of similar silica monoliths with ultra large (20–50 μm) macropores, but activated with sulphonic acid groups, in the esterification of acetic acid and lactic acid with *n*-butanol. While considered here as model reactions [21–25], they are both of a major practical interest. The *n*-butyl acetate is commonly used as a solvent in the manufacturing of lacquer, artificial perfume, photographic films, plastics and safety glass, and also as synthetic fruit flavouring in foods [26]. Typically, the esterification of lactic acid is applied to recover and purify the acid obtained by bacterial fermentation of carbohydrates [27,28]. But as all previous experiments with the reactors of this type were carried out in relatively benign conditions [7,20], we considered it also important to test whether they can effectively operate at elevated temperature.

2. Experimental part

2.1. Synthesis of silica monoliths

Silica rods of 4.5 mm diameter were synthesized using Nakanishi method [9–11] with the modifications described in [15,16]. In brief, 0.91 g of polyethylene glycol (PEG 35000) was dissolved in 10.5 cm^3 of 1 M HNO_3, next 7.6 cm^3 of TEOS was added slowly, followed by addition 0.4 g of cetyltrimethylammonium bromide (CTAB). The solution was mixed at room temperature for 1 h and then polypropylene tubes (5.7 mm i.d.) were filled with the sol. After gelation at 40 °C (12 h) they were aged at the same temperature for seven days. Then the samples were treated in 1 M ammonia aqueous solution at 90 °C for 9 h and after washing with water the monoliths were dried at 40 °C for three days and finally calcined at 550 °C for 5 h. During the processing shrinkage of about 20% of the size of mold was observed.

Single rods (1, 2 and 4 cm long) were embedded into a heat-shrinkable PTFE tubes (DSG-Canusa), equipped with connectors to obtain microreactors suitable for a continuous-flow operation. Then these microreactors were functionalized under flow (48 h, 60 °C) with arenesulphonic acid groups using solutions of 2-(4-chlorosulfonylphenyl)ethyltrimethoxysilane (CSPTMS; 50 wt% solution in CH_2Cl_2) dissolved in anhydrous ethanol (99.6%) to prevent uncontrolled hydrolysis.

2.2. Characterization of materials

Macropore structure of the monoliths thus obtained was investigated by mercury porosimetry (Quantachrome, PoreMaster 60), and by scanning electron microscopy (SEM, TM 30000 Hitachi). Low temperature nitrogen sorption (ASAP Micromeritics 2010) was applied to evaluate specific surface area (S_{BET}), mesopore volume and mesopore size distribution using desorption branch of isotherm and BJH method. Before analysis the samples were degassed for 24 h at 200 °C. The incorporation of functional groups was confirmed by FT-IR analysis (samples were prepared by KBr technique). Thermal properties and an amount of incorporated active groups were determined by thermogravimetric method (Mettler Toledo STAR 850). The weight loss and thermal effects during heating with ramp of 10 deg/min and air flow of 60 cm^3/min were recorded in the range of 25–800 °C. Additionally, drop pressure was measured in the continuous reaction conditions using pressure controller (UNIK 5000, Ex-Calibra).

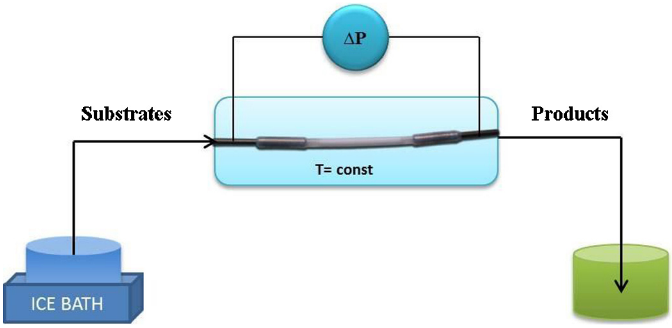

Fig. 1. Scheme of microreactor setup.

2.3. Catalytic measurements

The microreactor was tested in esterification of acetic acid and lactic acid with *n*-butanol (pure p.a, Chempur, Poland). The reactor setup is shown schematically in Fig. 1. The substrates solution was stored in ice bath to prevent any further reaction.

The experiments with acetic acid were performed for the molar ratio of substrates 1:1, at 75 °C using flow rates of 0.03, 0.06 and 0.09 cm^3/min. Esterification of lactic acid was carried out at 120 °C and 140 °C (measured with accuracy of ±0.1 °C) with flow rates of 0.03–0.4 cm^3/min. The molar ratio of lactic acid to *n*-butanol was 1:12, 1:6 and 1:1. The reaction progress was evaluated from the amount of acetic/lactic acid in the mixture. Acid concentration at the inlet and outlet of the microreactor was measured by titration method and additionally confirmed by gas chromatography (Agilent 7890 A, FID detector, HP-5 column).

Productivity of the microreactor and residence time was calculated from Eq. (1) and (2) [29]:

$$P = C_0 \times \mathrm{Conv} \times \frac{V_T}{\tau} \tag{1}$$

$$\tau = \frac{V_T \times m}{F} \tag{2}$$

where C_0 is initial concentration of substrate [$mmol/cm^3$], Conv is the conversion coefficient, V_T is the total pore volume [cm^3/g], τ is the residence time [min], m is the mass of monolith [g], F is the flow rate [cm^3/min]. The esterification of acetic acid was also carried out in batch reactor using round bottom flask (75 cm^3) equipped with a heating jacket and condenser. The reaction was performed under agitation at 1000 rpm using the same temperature and molar ratio of substrates as in the continuous process. The functionalized monolith was crushed and particles of ca. 50 μm were applied as catalyst at concentration of 0.74 wt%.

3. Results and discussion

Crack free silica rods displayed in Fig. 2 featured three types of pores detected by mercury porosimetry, nitrogen adsorption and scanning electron microscopy: (i) small mesopores with diameters ca. 3 nm and larger ones with maximum at 20 nm, originating from the presence of CTAB micelles, applied as soft pore templates, and a hydrothermal treatment of monoliths in ammonia solution, and (ii) ultra large macropores (flow-through channels) with diameters in the range of 20–50 μm (Figs. 3 and 4) obtained by

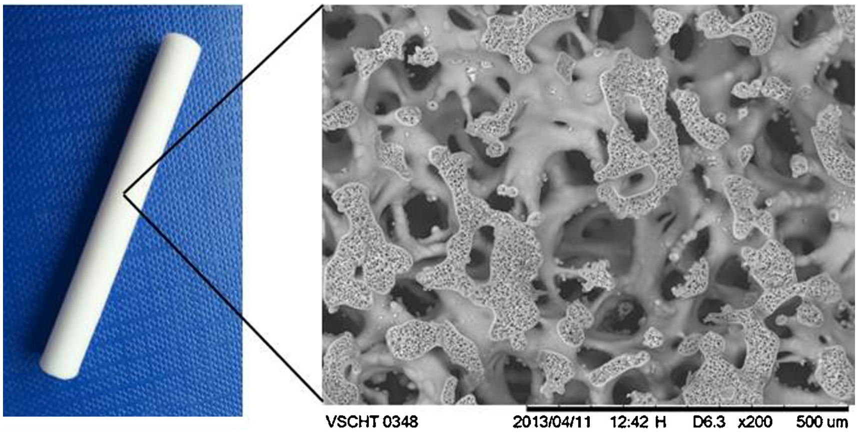

Fig. 2. Silica monoliths and SEM image of their structure.

Table 1
Texture parameters of monoliths.

Description	S_{BET} (m^2/g)	V_{mes} (cm^3/g)	V_{mac} (cm^3/g)	V_{total} (cm^3/g)	d_{mes} (nm)	d_{mac} (nm)
Monolith (M)	328	1.15	2.45	3.5	3.5/20	20–50
Functionalized monolith (MF)	245	0.91	2.45	3.25	20	20–50
Monolith after reaction (MFR)	275	0.91	2.44	3.25	20	20–50

PEG-induced phase separation. The bi-continuous structure of voids (macropores) and silica struts is well seen in the SEM image displayed in Fig. 2. Separated spherical voids of ca. 1 μm could also be observed in the silica skeleton, yet they were hardly detected by mercury porosimetry owing to their inaccessibility (Fig. 4). We believe that they originate from small PEG droplets. A pristine monolith (M) exhibited surface area of about 328 cm^2/g and mesopore volume of 1.15 cm^3/g (Table 1). After its functionalization with arenesulphonic groups (MF) smaller mesopores disappeared and this can be explained by a preferential deposition of functional groups' precursor in that space [30]. Clearly, it resulted in a decrease of specific surface area (ca. 17%). The monoliths thus obtained appeared to possess larger meso- and macropores compared to those reported before [6–8].

The presence of arenesulphonic groups on the monoliths' surface was investigated by FT-IR spectroscopy to obtain the spectra shown in Fig. 5. In all materials the asymmetric and symmetric stretching vibrations of the Si—O—Si framework occur in the range of 1000–1250 cm^{-1} and also 800 and 470 cm^{-1}. Weak absorption peak at around 960 cm^{-1} is attributed to stretching vibration of Si—OH group. Broad band in the range of 3000–3700 cm^{-1} corresponds to asymmetric stretching of hydrogen bonded OH groups. In the arenesulphonic-functionalized samples typical absorption bands from aromatic ring are observed at 700 cm^{-1}, 1403 cm^{-1}

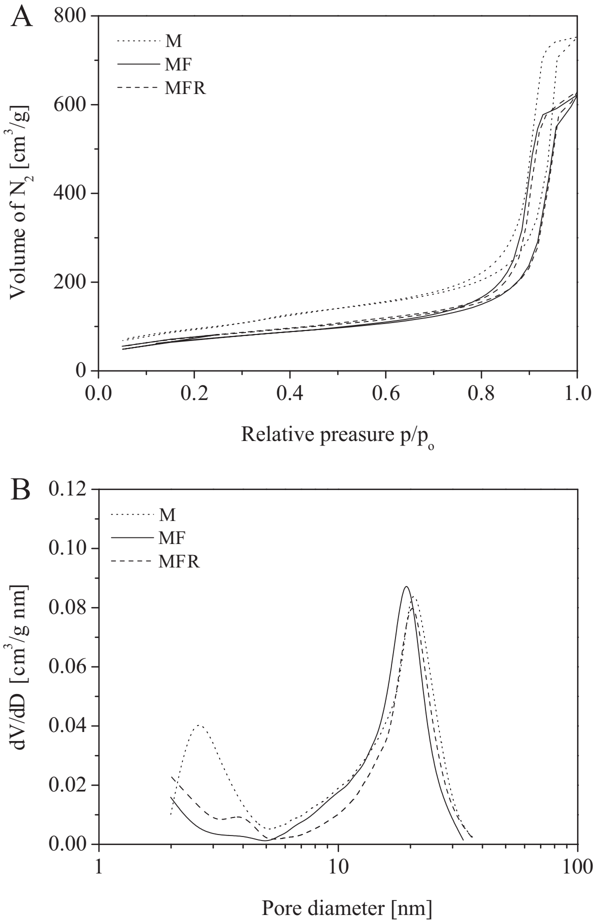

Fig. 3. Nitrogen adsorption/desorption isotherms (A) and pore size distributions (B) of pristine monolith (M), after its activation (MF) and after 3-day operation (MFR).

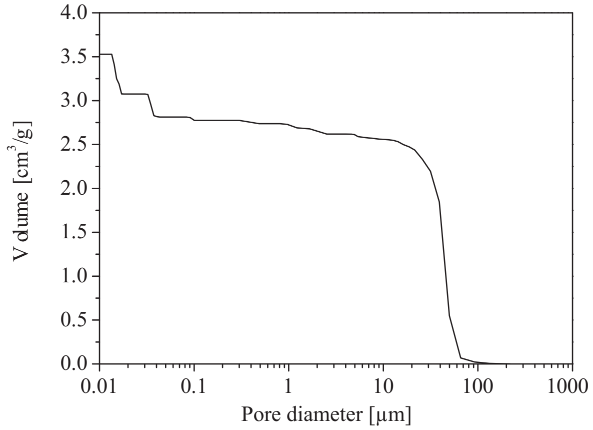

Fig. 4. Cumulative pore size distribution in a pristine monolith obtained by mercury porosimetry.

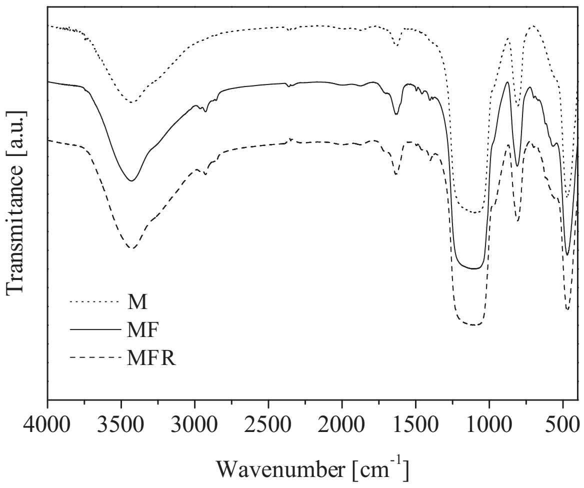

Fig. 5. FT-IR spectra of M, MF and MFR samples (the spectra were shifted for clarity).

and 1498 cm^{-1}. Absorption in the range of 2850–3000 cm^{-1} and the peak at 1457 cm^{-1} can be assigned to asymmetric stretching and bending vibration of C—H in methylene group connecting the aromatic ring. The S═O stretching vibrations of sulphonic groups normally occur in the range of 1000–1200 cm^{-1}. In the case of silica-based materials those vibrations overlap with Si—O—Si bands.

The amount of functional groups attached to the monoliths' surface and also their thermal stability were determined by thermal analysis. TG curves of the samples activated with different amounts of acidic groups are shown in Fig. 6A. Two steps of weight loss are clearly visible on the TG curve, especially from the sample with the largest content of functional groups. The sharp weight loss below 120 °C is assigned to the removal of physisorbed water, whereas the loss between 350 and 600 °C, corresponds to the decomposition of organic groups. Desorption of water and decomposition of organics appeared to be portrayed by two thermal effects; the endothermic peak with maximum at 100 °C and the exothermic (550 °C), are well seen on SDTA curve (Fig. 6B). The amount of incorporated groups was calculated from mass loss in the range of 350–600 °C and the values obtained were 0.15, 0.25 and 0.65 mmol/g. The largest value is consistent with the reported dependence between the maximum number of organic group, which could effectively be bound, and the concentration of hydroxyl groups present on the silica surface [31,32].

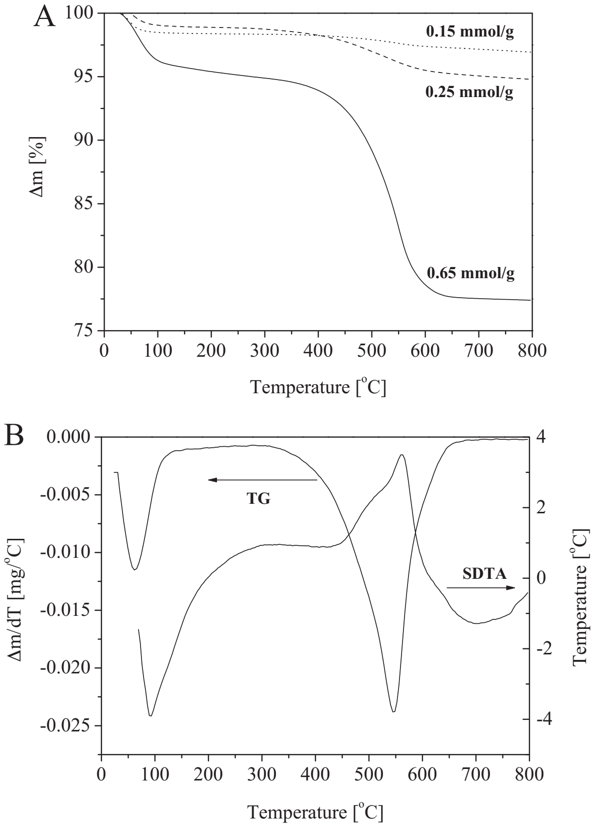

Fig. 6. TG curves of samples with different amount of incorporated acidic groups (A) and DTG and SDTA curves recorded for MF with 0.65 mmol/g of active groups (B).

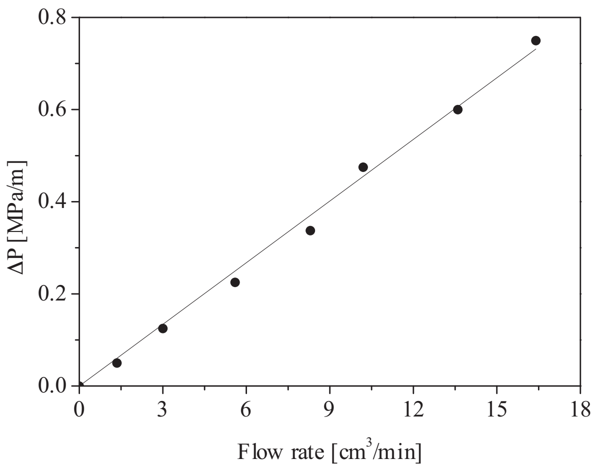

Fig. 7. Drop pressure vs. flow rate for 4 cm microreactor.

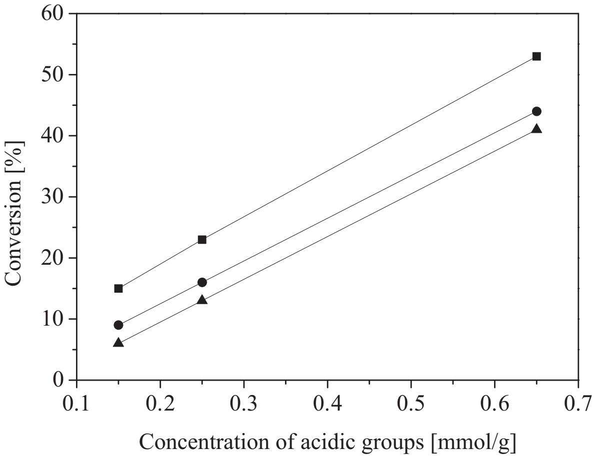

Fig. 8. Conversion of acetic acid vs. concentration of acidic groups for different flow rates: (■) 0.03 cm^3/min; (●) 0.06 cm^3/min and (▲) 0.09 cm^3/min.

For the continuous-flow microreactors the relationship between pressure drop and the flow rate through the monoliths is of practical significance. As can be inferred from Fig. 7, which shows the effect of liquid flow rate on pressure drop in the 4-cm reactor, the pressure drop in this microreactor was significantly smaller than that recorded before [7], due to the presence of much larger flow-through channels. This eliminates the need for the use of high-pressure metering pumps, typically applied in columns packed with fine beads, with a positive effect on process economy.

As indicated, catalytic properties of the microreactor were investigated in the esterification of acetic acid and lactic acid with *n*-butanol. First, the relationship between the amount of acidic groups and conversion was checked in esterification of acetic acid, at

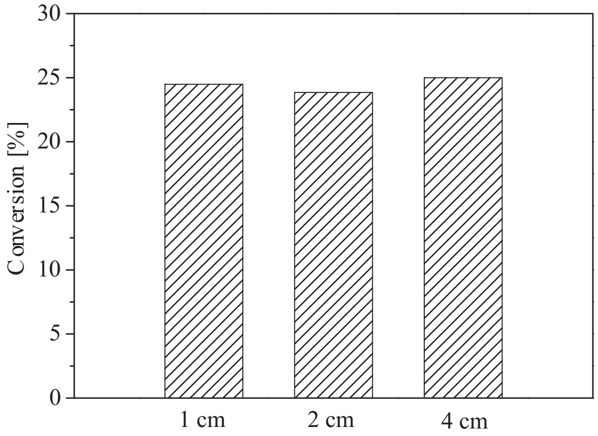

Fig. 9. Conversion of acetic acid in microreactors of different length for the residence time equal 155 s.

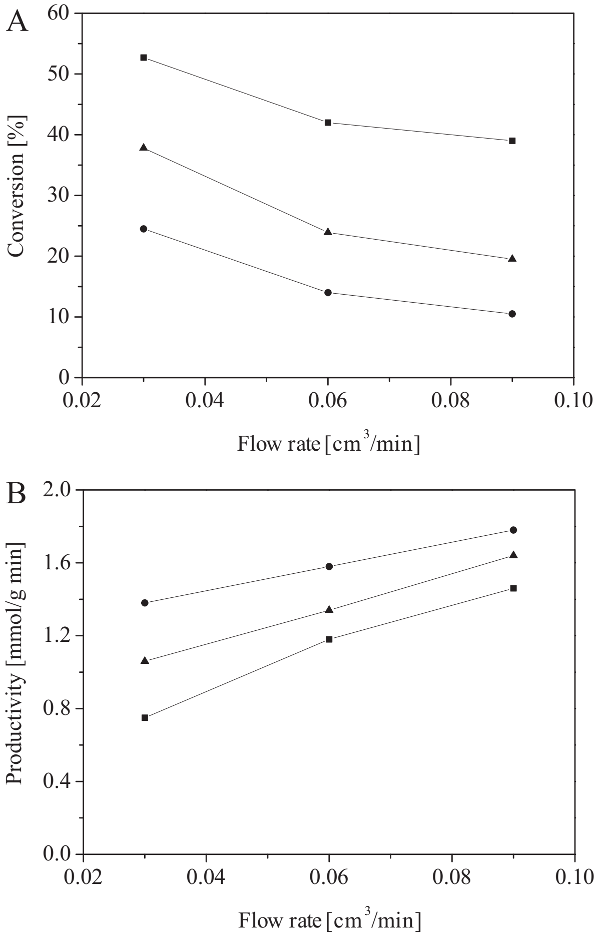

Fig. 10. Conversion of acetic acid (A) and productivity of ester (B) vs. flow rate in microreactors 1 cm (●), 2 cm (▲) and 4 cm (■) long.

different flow rates, to find a linear dependence (Fig. 8). Therefore, the bulk of experiments were performed for the monoliths with the highest concentration of acid groups, i.e. 0.65 mmol/g.

In order to check and eliminate the effect of external mass transfer on reaction kinetics, the reactors of different lengths were compared for the same residence time (155 s) to obtain similar values of conversion (ca. 25%, cf. Fig. 9); a clear proof of the lack of those limitations.

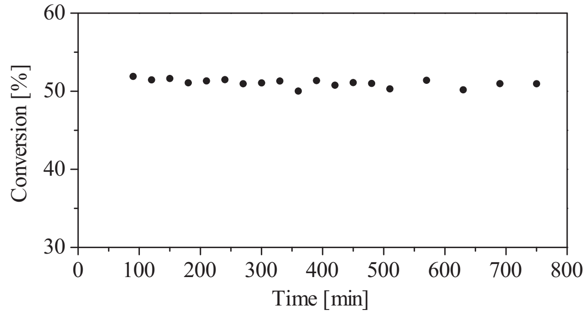

Fig. 11. Catalytic stability of microreactor in esterification of acetic acid with *n*-butanol (reaction conditions: 75 °C, molar ratio 1:1, flow rate 0.03 cm^3/min).

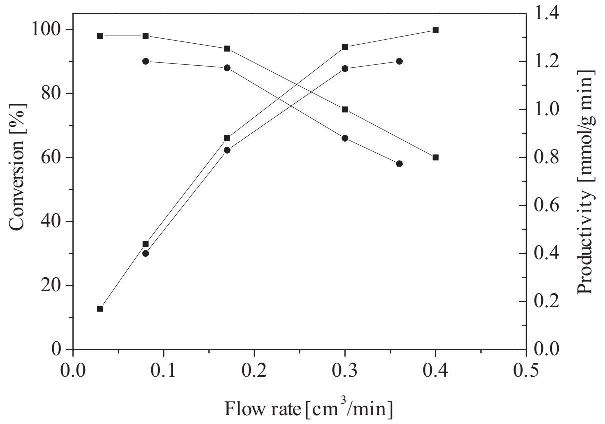

Fig. 12. Conversion of lactic acid and productivity of ester vs. flow rate in reactions carried out at (■) 140 °C and (●) 120 °C.

Fig. 10 shows the relationship of ester productivity and conversion of acetic acid against the flow rate for microreactors of different length (1–4 cm). As can be seen, the highest productivity (1.78 mmol/g min) was achieved in the shortest one (1 cm) and for the largest value of flow rate (0.09 cm^3/min), and this is in accord with expectations. An opposite relationship was observed for the case of conversion; the highest value, of ca. 53%, was received for 4 cm reactor and the lowest value of flow rate.

The performance of the monolithic and batch reactors was compared under identical conditions: the catalysts of 0.1444 g load, had either the form of monolith or powder, reaction time was 6 h and the volume of substrates was 21.6 cm^3. The conversion of acid was found to be ca. 42.5% and the productivity of ester reached the value of 1.2 mmol/g min in the both cases. This confirms that diffusion had no effect on the rate of reaction, unlike observed before for Diels–Alder reaction study, in which productivity in batch reactor was only half of that determined for the flow system [29]. But not less importantly, good catalytic stability during 800 min-long process was observed (Fig. 11).

To check the possibility of application these microreactors under more severe conditions, the esterification of lactic acid with *n*-butanol was performed. The results shown in Figs. 12 and 13 demonstrate almost full (99%) conversion of the acid when the process was carried out at 140 °C, the molar ratio of lactic acid to *n*-butanol equalled to 1:12 and the flow rate was in the range of 0.03–0.15 cm^3/min. This conversion is similar to that reported for batch process carried out over TiO_2–Al_2O_3 catalyst under the same conditions [24]. However, the productivity obtained in the monolithic microreactor under study (for flow rate of 0.15 cm^3/min) reached the value of 0.874 mmol/g min, i.e. four times more than reported. The increase in the flow rate to 0.3 cm^3/min decreased the conversion to 75%, but productivity increased by ca. 50%, to

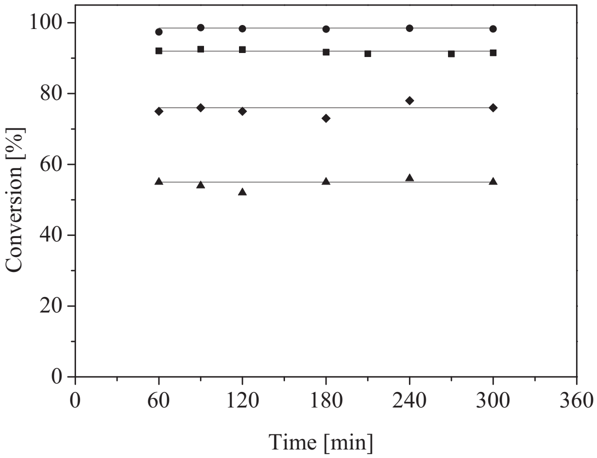

Fig. 13. Conversion of lactic acid vs. time at different reaction conditions: (●) 140 °C, 1:12; (■) 120 °C, 1:12; (♦) 120 °C, 1:6; (▲) 140 °C, 1:1.

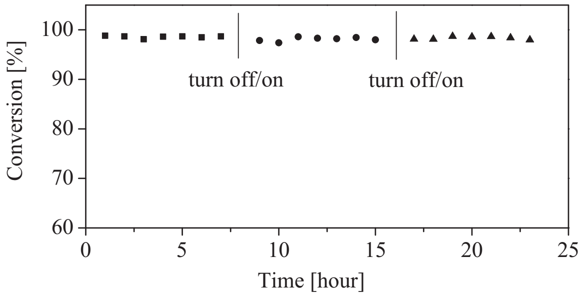

Fig. 14. Catalytic stability of microreactor in esterification of lactic acid with *n*-butanol: (■) 1st; (●) 2nd; (▲) 3rd day (reaction conditions: 140 °C, molar ratio 1:12, flow rate 0.15 cm^3/min).

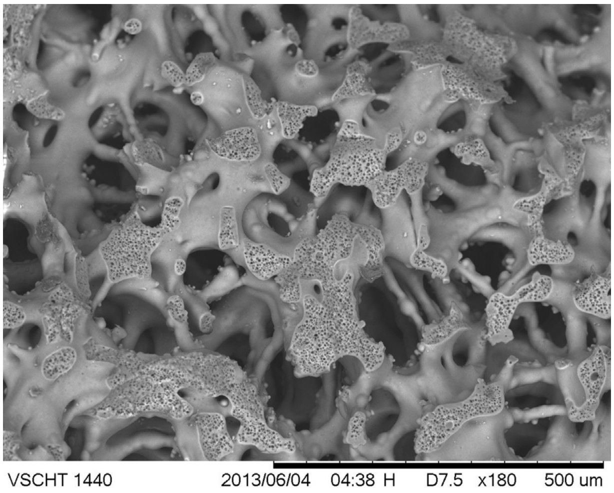

Fig. 15. SEM image of MFR monolith after esterification of lactic acid (reaction conditions: 140 °C, molar ratio 1:12, flow rate 0.15 cm^3/min).

the value of 1.25 mmol/g min. Further increase in the flow rate had a small affect on the increase of productivity. At lower temperature (120 °C) and with less excess of *n*-butanol (1:6 and 1:1) the efficiency of esterification was smaller, owing to reverse reaction effect.

The stability of microreactor was checked during three-day operation, discontinued for nights, to find that microreactor's performance did not change after the breaks (Fig. 14). The structure of the monolith also appeared to be well preserved both at the nanometric (Fig. 3) and micrometric scale (Fig. 15) and no change in the acidic groups content was detected by IR and thermogravimetric analysis after that period (data not shown).

4. Conclusions

A facile procedure to prepare an effective continuous-flow monolithic silica microreactor functionalized with arenesulphonic acid groups was proposed. Due to the presence of flow-through pores of 20–50 μm sizes these reactors can operate at low pressure drops which eliminate the need for the use of high pressure pumps. The relatively large specific surface area, ca. 250 m^2/g, exhibited by mesopores of ca. 20 nm present in silica skeleton allowed to attaching acidic groups in amount of 0.65 mmol/g. The microrector demonstrated very high activity and productivity and also good stability of catalytic and structural properties in the continuous esterification of acetic and lactic acid with *n*-butanol, even carried out at the temperature as high as 140 °C.

Acknowledgements

The support of the National Science Center for this project under the project UMO-2011/01/B/ST8/03855 is gratefully acknowledged.

References

[1] A. Stankiewicz, Chem. Eng. Sci. 56 (2001) 359–364.
[2] T.-H. Yoon, L.-Y. Hong, D.-P. Kim, Chem. Eng. J. 167 (2011) 666–670.
[3] J.F. Ng, Y. Nie, G.K. Chuah, S. Jaenicke, J. Catal. 269 (2010) 302–308.
[4] C. Viklund, F. Svec, J.M. Fréchet, K. Irgum, Chem. Mater. 8 (1996) 744–750.
[5] A. Cybulski, J.A. Moulijn, Catal, Rev. Sci. Eng. 36 (1994) 179–270.
[6] A. El Kadib, R. Chimenton, A. Sachse, F. Fajula, A. Galarneau, B. Coq, Angew. Chem. Int. Ed. 48 (2009) 4969–4972.
[7] A. Sachse, A. Galarneau, F. Fajula, F. Di Renzo, P. Creux, B. Coq, Microporous Mesoporous Mater. 140 (2011) 58–68.
[8] A. Sachse, A. Galarneau, B. Coq, F. Fajula, New J. Chem. 35 (2011) 259–264.
[9] K. Nakanishi, H. Minakuchi, N. Soga, N. Tanaka, J. Sol-Gel Sci. Technol. 13 (1998) 163–169.
[10] K. Nakanishi, Y. Kobayashi, T. Amatani, K. Hirao, T. Kodaira, Chem. Mater. 16 (2004) 3652–3658.
[11] N. Tanaka, H. Kobayashi, K. Nakanishi, H. Minakuchi, N. Ishizuka, Anal. Chem. 73 (2001) 420A–429A.
[12] A. Galarneau, J. Iapichella, K. Bonhomme, F. Di Renzo, P. Kooyman, O. Terasaki, F. Fajula, Adv. Funct. Mater. 16 (2006) 1657–1667.
[13] T. Martin, A. Galarneau, F. Di Renzo, F. Fajula, D. Plee, Angew. Chem. Int. Ed. 41 (2002) 2590–2592.
[14] J.H. Smått, S. Schunk, M. Linden, Chem. Mater. 16 (2003) 2354–2361.
[15] W. Pudło, W. Gawlik, J. Mrowiec-Białoń, T. Buczek, J.J. Malinowski, A.B. Jarzębski, Inż. Chem. Proc. 27 (2006) 177–185 (in Polish).
[16] A. Chrobok, S. Baj, W. Pudło, A.B. Jarzębski, Appl. Catal., A: Gen. 366 (2009) 22–28.
[17] A. Chrobok, S. Baj, W. Pudło, A.B. Jarzębski, Appl. Catal., A: Gen. 389 (2010) 179–185.
[18] A. Drożdż, A. Chrobok, S. Baj, K. Szymańska, J. Mrowiec-Białoń, A.B. Jarzębski, Appl. Catal., A: Gen. 467 (2013) 163–170.
[19] F. Hoffmann, M. Cornelius, J. Morell, M. Fröba, Angew. Chem. Int. Ed. 45 (2006) 3216–3251.
[20] K. Szymańska, W. Pudło, J. Mrowiec-Białoń, A. Czardybon, J. Kocurek, A.B. Jarzębski, Microporous Mesoporous Mater. 170 (2013) 75–82.
[21] B. Rabindran Jeremy, A. Pandurangan, J. Mol. Catal. A: Chem. 237 (2005) 146–154.
[22] G. Mitran, É. Makó, Á. Rédey, Catal. Lett. 140 (2010) 32–37.
[23] E. Sert, F.S. Atalat, React. Kinet. Catal. Lett. 99 (2010) 125–134.
[24] K.-T. Li, Ch.-K. Wang, Appl. Catal., A: Gen. 433–434 (2012) 275–279.
[25] K.-T. Li, Ch.-K. Wang, I. Wang, Ch.-M. Wang, Appl. Catal., A: Gen. 392 (2011) 180–183.
[26] Data K., in: Encyclopedia of Chemical Technology, Wiley, New York, 13 (1997) 1042-1058.
[27] D. Garlotta, J. Polym. Environ. 9 (2001) 63–84.
[28] S.P. Kamble, P.P. Barve, J.B. Joshi, I. Rahman, B.D. Kulkarni, Ind. Eng. Chem. Res. 51 (2012) 1506–1514.
[29] A. Sachse, V. Hulea, A. Finiels, B. Coq, F. Fajula, A. Galarneau, J. Catal. 287 (2012) 62–67.
[30] A. Zuka, H. Silklova, J. Cejka, Langmuir 24 (2008) 9837–9842.
[31] J. Mrowiec-Białoń, Thermochim. Acta 443 (2006) 49–52.
[32] L.T. Zhuravlev, Colloids Surf., A: Physicochem. Eng. Aspects 173 (2000) 1–38.